

Entropy Consistent Methods for the Navier–Stokes Equations

A First-Order Systems Approach

Akmal Nizam Mohammed · Farzad Ismail

Received: 3 December 2013 / Revised: 3 July 2014 / Accepted: 13 August 2014 /
Published online: 23 August 2014
© Springer Science+Business Media New York 2014

Abstract The concept of entropy conservation, stability, and consistency is applied to systems of hyperbolic equations to create new flux functions for the scalar and systems of conservation laws. Firstly, Burgers' equation is modelled, followed by the Navier–Stokes equations. The new models are compared with the pre-existing entropy consistent fluxes at selected viscosity levels; it is found that the system flux requires additional entropy production at low viscosities, but not at higher viscosity values. Initial results herein demonstrate that the accuracy of the first order systems approach are comparable to the results produced by the original entropy-consistent Navier–Stokes flux.

Keywords Shock capturing · Navier–Stokes flux · Entropy consistency · Entropy production · First-order systems

1 Introduction

Even now, diffusion via entropy generation is still an underdeveloped facet of the shock capturing scheme. Since the elucidation of the entropy stability concept in Tadmor [17], the deployment of entropy control as an additional constraint to the governing equations of fluid flow has been widespread. These include the work of Fjordholm et al. [2,3,5]. Amongst the various schemes that apply such a method, the entropy consistent flux formulation available originally in Roe [16] (revised in Ismail [7]) and further extended in Ismail and Roe [8] remains an interesting proposition for its low cost and stability, as shown subsequently in

A. N. Mohammed
Faculty of Mechanical and Manufacturing Engineering, Universiti Tun Hussein
Onn Malaysia, Batu Pahat, Malaysia
e-mail: akmaln@uthm.edu.my

A. N. Mohammed · F. Ismail (✉)
School of Aerospace Engineering, Engineering Campus, Universiti Sains Malaysia,
Penang, Malaysia
e-mail: aefarzad@usm.my

Kitamura et al. [9]. However, this flux function still has room for improvement, since the amount of entropy actually generated particularly when solving the Navier–Stokes equations may differ from the entropy production predicted by the Euler flux as found in Mohammed and Ismail [11]. Therein, it is shown that the entropy–stability term alone is sufficient for most physical viscosity values, and that the entropy consistency (third term) is only needed for relatively low viscosity values (high Reynolds number flow). Despite this, it would make sense to continue the search for a ‘truer’ means of modelling diffusion, using more of physical viscosity such as in Tadmor and Zhong [18, 19] to facilitate entropy generation and less dependent on artificial viscosity methods.

1.1 Entropy Conservation, Entropy–Stability and Entropy–Consistency

Following [8], for any hyperbolic system of conservation laws satisfying:

$$\mathbf{u}_t + \mathbf{f}_x = 0 \tag{1}$$

or in integral form

$$\oint (\mathbf{u}dx - \mathbf{f}dt) = 0 \tag{2}$$

there is an additional entropy U constraint satisfying

$$U_t + F_x \leq 0 \tag{3}$$

with the integral form

$$\oint (Udx - Fdt) \leq 0 \tag{4}$$

The inequality is to cater for discontinuous flow where entropy is produced. Note that entropy is conserved for smooth flows thus equality is achieved. For ideal gas dynamics, the entropy pair (U, F) that can be used for both the Euler and Navier–Stokes equations [6] only if $U = -\frac{\rho S}{\gamma-1}, F = -\frac{\rho u S}{\gamma-1}$ where $S = \ln p - \gamma \ln \rho$ is the physical entropy. The negative sign in U is a mathematical convention to ensure that the entropy satisfying Eq. (3) is decreasing which is the opposite to the nature of physical entropy. Alternatively, the entropy production in a domain Ω with boundary $\partial\Omega$ can be written as

$$\dot{U} = \int \int_{\Omega} (U_t + F_x) dxdt = \oint_{\partial\Omega} (Udx - Fdt) \tag{5}$$

for which $\dot{U} = 0$ implies entropy conservation and that $\dot{U} < 0$ denotes entropy is decreasing (or entropy–stable).

In a discrete form of the governing equations, the conservation laws of Eq. (2) must be satisfied and that zero entropy production must be observed for smooth flows. A discrete approach satisfying this proposition is deemed as an entropy–conserved method. On the other hand, a discrete method solving Eq. (2) is defined as entropy–stable if it always produces a decreasing entropy production. Entropy–stability however, only guarantees that the discrete approach produces the correct sign of entropy production but not necessarily the correct amount. If a discrete approach produces the “correct” amount of entropy generation, then it is defined as an entropy–consistent method. Achieving entropy–conservation and entropy–stability are quite straightforward since they are both enforced locally within a cell as will be shown in Sects. 2 and 3. Unfortunately, that is not the case for entropy-consistency since shocks will be captured over several cells and the required total entropy have to be generated over more than one cell. Unlike entropy conservation, the problem is no longer local thus

it is quite hard in general to determine the precise amount of entropy generation. Too much of entropy generation would cause a smearing of the discontinuous profile while too little entropy production would give rise to oscillatory behavior around the discontinuity. To the authors' best knowledge, there is yet a solid analytical relation between entropy production and shock quality although some form of approximation model has been done for the inviscid approach in Ismail and Roe [8]. Thus, all we seek is just a "sensible" shock profile and that much of the work herein relies on numerical experiment to achieve entropy-consistency.

1.2 Advantages of the First-Order System

A major obstacle in incorporating physical viscosity lies in the nature of its high-order relationship with other conserved variables. This leads to a difficulty of the inviscid part of the governing equation having a hyperbolic basis, and the viscous part with its parabolic affinity. An answer for this quandary is tackled through the deployment of first-order system fluxes, as shown in Nishikawa [12]. This line of thought has been continued through a series of articles in Nishikawa [13–15], amongst others. The advantages of this method include having a fully hyperbolized advection–diffusion model (i.e. leading to explicit time integration methods) and a faster rate of convergence, leading to relatively cheap costs. However, this method does have a limitation in that for transient problems, the additional hyperbolic equations which govern the viscosity would need to achieve steady-state before marching forward in time, and thus would require sub-iterations for each time step.

In this paper, the authors will attempt to combine the ideas of entropy–stability (and consistency) with the concept of the first-order system, with the hope of harnessing the best of both methods. The newly synthesized fluxes are then applied to steady problems to observe the evolution of entropy in the pseudo-transient computation towards the steady state.

2 System Flux for Burgers' Equation

Consider the governing equation for advection and diffusion:

$$\mathbf{u}_t + \mathbf{f}_x = \nu \mathbf{u}_{xx} \quad (6)$$

A subset of this is the Burgers' equation, in which \mathbf{u} and \mathbf{f} are scalars:

$$u_t + f_x = \nu u_{xx}, \quad f_x = \left(\frac{u^2}{2} \right)_x \quad (7)$$

To discretize an entropy consistent flux based on this equation, a mapping from the conserved variables to the corresponding entropy equation is sought.

2.1 Entropy Conservative Flux

Following the work of Ismail and Roe [8], the inviscid part of the equation is discretized using a semi-discrete finite volume method, such that

$$\left(\frac{\partial u}{\partial t} \right)_j \Delta x = - \left(f_{j+\frac{1}{2}} - f_{j-\frac{1}{2}} \right) \quad (8)$$

where $f_{j\pm\frac{1}{2}} = f^*$ are the fluxes to be evaluated at the respective interfaces. In a dual-cell system, this equation can be viewed from a residual distribution approach thus split into two parts:

$$h_L \frac{\partial u_L}{\partial t} = f_L - f^* \tag{9a}$$

$$h_R \frac{\partial u_R}{\partial t} = f^* - f_R \tag{9b}$$

The variable h is the length of each cell, while the subscripts L and R denotes the left and right states respectively. In order to establish entropy conservation, a convex entropy function $U(u)$ is introduced, along with its associated entropy variable v , and an entropy flux $F(U)$ satisfying Eq. (4). We define $U = u^2$, $v = \frac{\partial U}{\partial u}$, and $F = \frac{2}{3}u^3$, and substitute the original variables in Eq. (9) with these terms, yielding:

$$h_L \frac{\partial U_L}{\partial t} = v_L(f_L - f^*) \tag{10a}$$

$$h_R \frac{\partial U_R}{\partial t} = v_R(f^* - f_R) \tag{10b}$$

To determine the change of entropy within each cell, the sum of both parts of Eq. (10) is required:

$$\begin{aligned} \frac{\partial}{\partial t}(h_L U_L + h_R U_R) &= (v_L f_L - v_R f_R) + (v_R - v_L) f^* \\ &= -[vf] + [v]f^* \end{aligned} \tag{11}$$

where $[v] = v_R - v_L$. Similarly, the total entropy change predicted by the entropy conservation law would be:

$$\frac{\partial}{\partial t}(h_L U_L + h_R U_R) = F_L - F_R = -[F]. \tag{12}$$

It is not guaranteed that each local entropy flux would always add up to the global entropy change. For the correct physics of entropy to remain true, the change of the discrete fluxes in Eq. (11) should at least be a match to the fluxes in Eq. (12), and the difference between the two quantities must be accounted for in the form of the entropy production \dot{U} as stated in Eq. (5) [16]:

$$\dot{U} = [F] + ([v]f^* - [vf]). \tag{13}$$

To get a conservative flux, f^* can be chosen so that the local and system entropy fluxes balance out exactly. For Burgers’ equation, $f = \frac{1}{2}u^2$, producing the entropy conserved flux f_c^*

$$f_c^* = \frac{1}{6} (u_L^2 + u_R u_L + u_R^2) \tag{14}$$

2.2 Entropy–Stable and Entropy–Consistent Fluxes

However, as mentioned in Sect. 1.1, only having conservation may not be enough, since entropy would naturally occur for all irreversible processes. Hence, more are built into the flux, leading to the *entropy consistent* form recommended in Ismail and Roe [8]:

$$f^* = f_c^* - \frac{1}{2} (|\bar{a}| + \alpha|[a]) [u] \tag{15a}$$

$$= f_c^* - \frac{1}{2} (|\bar{a}| + \alpha|[a]) \frac{du}{dv} [v] \tag{15b}$$

Using Eq. (13), the entropy generation thus becomes

$$\dot{U} = -\frac{1}{2}(|\bar{a}| + \alpha|a|)\frac{du}{dv}[v]^2 \leq 0. \tag{16}$$

In this equation, \bar{a} is the arithmetic averaging of velocity at the interface having left and right cell values, whilst α is an analytically determined parameter [8]. Notice that the production term is made up of components that are invariably positive. Considering its entropy conservative nature, the fact that the entropy production would always have the correct sign means the flux definitely satisfies the entropy inequality of Eq. (4). The flux is deemed entropy consistent by virtue of producing enough entropy, both artificially generated by the inviscid flux and physically sourced by the discrete viscous part of Burgers’ equation usually via central differencing. Thus, the overall entropy production for the flux of Eq. (15) depends only on the physical and numerical viscosities:

$$\begin{aligned} \dot{U} &= -\frac{1}{2}(|\bar{a}| + \alpha|a|)\frac{du}{dv}[v]^2 - \frac{\nu}{\Delta x}[u][v] \\ &= -\frac{1}{2}(|\bar{a}| + \alpha|a|)\frac{du}{dv}[v]^2 - \frac{\nu}{(2\Delta x)}[v]^2 \end{aligned} \tag{17}$$

The diffusive term is constructed based on a generalized expression for physical viscosity (from Eq. 7), which is then discretized and multiplied by $[v]$ to map it as entropy production. Again $\dot{U} \leq 0$, satisfying the entropy inequality.

2.3 First-Order Hyperbolic System

The Burgers’ equation can be written in the alternative form of a first-order system:

$$\mathbf{u}_t + \mathbf{f}_x = \mathbf{q} \tag{18}$$

The vectors are defined as:

$$\mathbf{u} = \begin{bmatrix} u \\ d \end{bmatrix}, \quad \mathbf{f} = \begin{bmatrix} u^2/2 - \nu d \\ -u/T_r \end{bmatrix}, \quad \mathbf{q} = \begin{bmatrix} 0 \\ -d/T_r \end{bmatrix} \tag{19}$$

with $d = \frac{\partial u}{\partial x}$. The quantity T_r is the relaxation time. The eigenvalues for the system of equations satisfying (18) and (19) are

$$\mathbf{\Lambda} = \begin{bmatrix} \lambda_1 & 0 \\ 0 & \lambda_2 \end{bmatrix}, \quad \lambda_{1,2} = \frac{1}{2} \left(u \pm \sqrt{u^2 + 4\frac{\nu}{T_r}} \right) \tag{20}$$

representing the characteristic waves speeds for u, d . These eigenvalues can be stated as:

$$\lambda_1 = \frac{1}{2} \left(u_1 + \sqrt{(u_1)^2 + 4\frac{\nu}{T_r}} \right), \quad \lambda_2 = \frac{1}{2} \left(u_2 - \sqrt{(u_2)^2 + 4\frac{\nu}{T_r}} \right) \tag{21}$$

where we have introduced two velocities (u_1, u_2) for discretization purposes as will be shown later in this subsection. Note that for $\nu = 0$, the eigenvalues reduces to just one nonzero quantity ($\lambda_1 = u$) which represents the pure transport of the inviscid Burgers equation.

The right eigenvectors R are defined as:

$$\mathbf{R} = \begin{bmatrix} -\lambda_1 T_r & -\lambda_2 T_r \\ 1 & 1 \end{bmatrix} \tag{22}$$

The value of T_r is proportional to $\frac{L_x^2}{\nu}$, and hence would have a low but finite value to reflect proximity to equilibrium conditions for diffusion, as opposed to frozen (high relaxation time).

After doing some manipulation of T_r , [13] presented an alternative set of eigenvalues and eigenvectors based on the local Reynolds number and relaxation length (L_r). However, from now onwards we shall assume that T_r is a constant number set to unity. This assumption will only remain valid for steady computations, as the accuracy of the hyperbolic system in modelling the original equation relies on the condition that the relaxation time is sufficiently small [12].

From this model, the aim is to obtain an entropy consistent flux function in the same vein as the scalar Burgers’ equation. To achieve this, we need to define an entropy function that has some measure of “total energy” based on the primary variable u and its auxiliary term d . We seek to control this “total energy” through the concept of entropy conservation, entropy stability and entropy consistency. Based on the work of [6], we define an entropy pair (U, F) :

$$\frac{\partial U}{\partial \mathbf{u}} \frac{\partial \mathbf{f}}{\partial \mathbf{u}} = \frac{\partial F}{\partial \mathbf{u}} \tag{23}$$

where

$$U = U_i + U_v = u^2 + \nu d^2, \quad F = F_i + F_v = \left(\frac{2}{3}u^3\right) - 2\nu u d \tag{24}$$

satisfying the entropy constraint given in Eq. 4. The entropy pair (U, F) are purposefully chosen to be convex functions so as to allow for one-to-one mapping. For $\nu = 0$, this governing entropy equation will collapse into the original entropy equation for the inviscid Burgers’ equation. The entropy variables are now defined as:

$$\mathbf{v} = \frac{\partial U}{\partial \mathbf{u}} = \begin{bmatrix} 2u \\ 2\nu d \end{bmatrix} \tag{25}$$

The total flux at the interface combines both the inviscid flux $\hat{\mathbf{f}}_i$ and the viscous flux $\hat{\mathbf{f}}_v$ in a discrete form that is originally derived in Barth [1] and modified to its current variation in Ismail and Roe [8]:

$$\mathbf{f}^* = \hat{\mathbf{f}}_i + \hat{\mathbf{f}}_v - \frac{1}{2} \hat{\mathbf{R}} |\hat{\Lambda} \hat{\mathbf{S}}| \hat{\mathbf{R}}^T [\mathbf{v}] \tag{26}$$

where the accented “^” variables represent discrete averaged quantities. The expression at the tail end of the right hand side of Eq. (26) is the dissipation matrix, whose job is to maintain the stability via proper entropy generation for the flux.

The scaling parameter \mathbf{S} is a diagonal matrix to the convert the numerical diffusion based on the wave-characteristics $\mathbf{R}\mathbf{A}\mathbf{R}^{-1}d\mathbf{u}$ into a numerical diffusion based on the entropy–variables \mathbf{v} , which is entropy–stable. The idea originally came from Barth [1]. At the differential level $\mathbf{R}\mathbf{A}\mathbf{R}^{-1}d\mathbf{u} = \mathbf{R}\mathbf{S}\mathbf{R}^T d\mathbf{v}$ is true as proven in Roe [16] and most recently in Fjordholm et al. [4]. \mathbf{S} is merely a multiplier to ensure proper mapping of numerical diffusion based on conserved variables to entropy–variables is analytically correct; the system’s eigenvalues and eigenvectors remain unchanged even with its addition [4]. Note that for a smooth flow, the numerical diffusion based on the entropy–variables similarly behaves to diffusion using the conserved–variables. The two approaches differ when the flow is non-smooth, and this is critical in terms of achieving proper entropy generation in which the entropy–variables approach is more physical. The scaling parameter \mathbf{S} is:

$$\hat{\mathbf{S}} = \begin{bmatrix} \frac{\hat{\lambda}_2^2 + \nu}{2\nu(\hat{\lambda}_1 - \hat{\lambda}_2)^2 + \epsilon} & -\frac{\hat{\lambda}_1 \hat{\lambda}_2 + \nu}{2\nu(\hat{\lambda}_1 - \hat{\lambda}_2)^2 + \epsilon} \\ -\frac{\hat{\lambda}_1 \hat{\lambda}_2 + \nu}{2\nu(\hat{\lambda}_1 - \hat{\lambda}_2)^2 + \epsilon} & \frac{\hat{\lambda}_1^2 + \nu}{2\nu(\hat{\lambda}_1 - \hat{\lambda}_2)^2 + \epsilon} \end{bmatrix} \tag{27}$$

A very small coefficient $\epsilon = 1.0 \times 10^{-10}$ has been added to the denominators to prevent the function from dividing by zero.

The discrete inviscid and viscous fluxes are arranged as:

$$\hat{\mathbf{f}}_i = \begin{bmatrix} u_1^{2*} \\ 0 \end{bmatrix}, \quad \hat{\mathbf{f}}_v = \begin{bmatrix} -\nu d^* \\ -u_2^* \end{bmatrix} \tag{28}$$

where the accent “*” denote the averaged interface values to be determined. Note that we have defined two averaged quantities for the velocities (u_1^*, u_2^*).

To achieve entropy conservation, recall how the scalar cell flux in Eq. (11) is equated to the total flux of Eq. (12). The procedure is now applied to the system’s approach, by replacing the scalar variables with vectors:

$$[\mathbf{v}]^T \mathbf{f}^* - [\mathbf{v} \cdot \mathbf{f}] = -[F]. \tag{29}$$

Note that this is an under-determined equation hence there will be more than one set of solutions. However, only one set of solutions are needed to explicitly determine the averaged quantities. The previous equation when expanded becomes

$$\begin{aligned} [2u] \frac{u_1^{2*}}{2} - 2\nu[u]d^* - 2\nu[d]u_2^* - [u^3] + 2\nu[ud] + 2\nu[ud] &= -\frac{2}{3}[u^3] + 2\nu[ud] \\ ([u]u_1^{2*} - [u^3]) + (2\nu[ud] - 2\nu[u]d^* - 2\nu[d]u_2^*) &= -\frac{2}{3}[u^3]. \end{aligned} \tag{30}$$

Using the identity $[ab] = \bar{a}[b] + \bar{b}[a]$, the equation reduces to

$$[u]u_1^{2*} + 2\nu(\bar{u}[d] + \bar{d}[u]) - 2\nu[u]d^* - 2\nu[d]u_2^* = \frac{1}{3}[u] (u_L^2 + u_L u_R + u_R^2). \tag{31}$$

By equating the terms on the left hand side to the right hand side of equation, the inviscid entropy conserved flux formulation is recovered, $u_1^* = \frac{1}{3}(u_L^2 + u_L u_R + u_R^2)$. And by choosing $u_2^* = \bar{u}$ and $d^* = \bar{d}$, the whole equation cancels out thus obtaining entropy conserved fluxes for the inviscid and viscous parts.

$$\hat{\mathbf{f}}_i = \begin{bmatrix} \frac{1}{6} (u_L^2 + u_L u_R + u_R^2) \\ 0 \end{bmatrix}, \quad \hat{\mathbf{f}}_v = \begin{bmatrix} -\nu \bar{d} \\ -\bar{u} \end{bmatrix}. \tag{32}$$

The total entropy production based on the flux discretization (f^*) in Eq. (26) and including the source terms is

$$\begin{aligned} \dot{U} &= [\mathbf{v}]^T \mathbf{f}^* - [\mathbf{v} \cdot \mathbf{f}] + [F] + \mathbf{v} \cdot \mathbf{q} \\ &= -\frac{1}{2}[\mathbf{v}]^T \hat{\mathbf{R}} |\hat{\Lambda} \hat{\mathbf{S}}| \hat{\mathbf{R}}^T [\mathbf{v}] - 2\nu d^2 \leq 0 \end{aligned} \tag{33}$$

which ensures that the entropy defined in Eq. (24) is decreasing since the product of the first term on the right hand side is a positive definite matrix and that the second term (representing the source terms) is always decreasing. Although the first order system is different from the conventional approach of advection-diffusion problem but the former still produces the proper entropy generation. Define

$$\hat{\mathbf{A}}_{ECS1} = \begin{bmatrix} \hat{\lambda}_1 & 0 \\ 0 & \hat{\lambda}_2 \end{bmatrix} \tag{34}$$

to represent the wave speeds for ECS1 method.

To achieve entropy–consistency, one viable approach is to utilize the analytically determined entropy–consistent method for Burgers equation recommended by Ismail and Roe [8]:

$$\hat{A}_{ECS2} = \begin{bmatrix} \hat{\lambda}_1 + \frac{1}{6}|\lambda_1| & 0 \\ 0 & \hat{\lambda}_2 + |\lambda_2| \end{bmatrix} \tag{35}$$

where herein stated as the ECS2 method.

3 Navier–Stokes System Flux

The first order system is then extended to the Navier–Stokes equations (without heat) in the manner prescribed by Nishikawa [14]. Consider the conservation law with source terms:

$$\mathbf{u}_t + \mathbf{f}_x = \mathbf{B} \tag{36}$$

where

$$\mathbf{u} = \begin{bmatrix} \rho \\ \rho u \\ \rho E \\ \tau \end{bmatrix}, \quad \mathbf{f} = \mathbf{f}_i + \mathbf{f}_v = \begin{bmatrix} \rho u \\ p_1 + \rho u^2 \\ \rho u H \\ 0 \end{bmatrix} + \begin{bmatrix} 0 \\ -\tau \\ -\tau u \\ -\frac{\mu_v}{T_v} u \end{bmatrix}$$

$$\mathbf{B} = \begin{bmatrix} 0 \\ 0 \\ 0 \\ -\frac{\tau}{T_v} \end{bmatrix}, \quad \tau = \frac{4}{3}\mu \frac{\partial u}{\partial x} \tag{37}$$

The heat transfer component is removed to concentrate on the effect of the viscous term. The scaled viscosity μ_v and the relaxation time T_v are defined in the following with subscript v denoting viscous stress:

$$\mu_v = \frac{4}{3}\mu, \quad T_v = \frac{L^2}{\nu_v}, \quad \nu_v = \frac{\mu_v}{\rho}. \tag{38}$$

L is a length scale, whilst ν_v is the kinematic viscosity. Similar to the Burgers’ equation in the previous section, the length scale and relaxation time mentioned here result in an approximation of the viscosity term only in steady state. Following Nishikawa [14], the first order system for Navier–Stokes equation can be rewritten as

$$\mathbf{P}^{-1} \frac{\partial \mathbf{u}}{\partial t} + \frac{\partial \mathbf{f}}{\partial x} = \mathbf{B}, \quad \mathbf{P}^{-1} = \begin{bmatrix} 1 & 0 & 0 & 0 \\ 0 & 1 & 0 & 0 \\ 0 & 0 & 1 & 0 \\ 0 & 0 & 0 & \frac{T_v}{\mu_v} \end{bmatrix}. \tag{39}$$

The matrix \mathbf{P} is a local preconditioning for the viscous stress. Since both \mathbf{P} and \mathbf{B} matrices affect only the auxiliary equations in the system, Eq. (39) can still be considered as conservative.

The next step is to construct an entropy function which depends on both the inviscid and viscous fluxes similar to the strategy used for the Burgers equation. Since $U = -\rho S/(\gamma - 1)$ is the only entropy function from Euler equations that can be extended to the Navier–Stokes equations [6], it is chosen to represent the inviscid fluxes. On the other side, the viscous entropy functions must be of the form of the viscous stresses (τ) and the temperature gradients (q). For this paper, we concentrate on the effects of viscosity by eliminating the influence of heat transfer from the system, meaning that $q = 0$. Overall, these entropy functions are defined as:

$$U_i = -\frac{\rho S}{\gamma - 1}, \quad U_v = \tau^2 + \rho u^2 \tag{40}$$

with its fluxes defined as

$$F_i = -\frac{\rho u S}{\gamma - 1}, \quad F_v = -2u\tau \tag{41}$$

where the viscous part for entropy measures some form of “energy” of the system. As before, the entropy pair (U, F) are convex functions [6]. However, unlike the Burgers equation in which entropy is viewed as one parameter consisting the summation of inviscid and viscous parts, the Navier–Stokes entropies are two different entities that are practically untied from each other. This is due to the philosophy espoused by Nishikawa [14] and adopted in this paper specifically for the Navier–Stokes model, which is to treat the inviscid and viscous portions of the equations as two independent entities in an interconnected hyperbolic system. Thus, defining the function and the fluxes in this way means that each type would only need to adhere to the entropy conditions of their own respective systems, one for the inviscid (physical) and the other for the viscous part. As such, both U_i and U_v independently satisfy the entropy inequality, and the constraint of the entropy pair theorem given in Eq. (23) from [6]. Following that, the entropy variables and its discrete fluxes are split into two separate parts:

$$\mathbf{v}_i = \frac{\partial U_i}{\partial \mathbf{u}}, \quad \mathbf{v}_v = \frac{\partial U_v}{\partial \mathbf{u}}, \quad \hat{\mathbf{f}} = \hat{\mathbf{f}}_i + \hat{\mathbf{f}}_v \tag{42}$$

The inviscid variables are defined as:

$$\mathbf{v}_i = \begin{bmatrix} \frac{\gamma - S}{\gamma - 1} & -\frac{1}{2} \frac{\rho u^2}{p} \\ \frac{\rho u}{p} \\ -\frac{\rho}{p} \\ 0 \end{bmatrix}, \quad \hat{\mathbf{f}}_i = \begin{bmatrix} \hat{\rho} \hat{u}_1 \\ \hat{p}_1 + \hat{\rho} (\hat{u}_1)^2 \\ \hat{\rho} \hat{u}_1 \hat{H} \\ 0 \end{bmatrix} \tag{43}$$

The flux $\hat{\mathbf{f}}$ consists of averaged quantities (denoted by the accent \hat{a} in general) that are to be determined by ensuring entropy is conserved. Similar to Eq. (29), entropy conservation requires

$$[\mathbf{v}_i]^T \hat{\mathbf{f}}_i - [\mathbf{v}_i \cdot \mathbf{f}_i] = -[F_i] \tag{44}$$

Using the identity $[\mathbf{v}_i \cdot \mathbf{f}_i] - [F_i] = [\rho u]$, the previous equation becomes

$$[\mathbf{v}_i]^T \hat{\mathbf{f}}_i = [\rho u] \tag{45}$$

By choosing the averaged quantities as given in “Appendix 1”, the discrete inviscid fluxes conserve the inviscid part of entropy U_i as shown in Ismail and Roe [8]. The remaining averaged quantity for the flux of τ is now determined, starting with the viscous entropy variables and discrete fluxes:

$$\mathbf{v}_v = \begin{bmatrix} -u^2 \\ 2u \\ 0 \\ 2\tau \end{bmatrix}, \quad \hat{\mathbf{f}}_v = \begin{bmatrix} 0 \\ -\tau^* \\ -\tau^* u_2^* \\ -\frac{\mu_v}{T_v} u_2^* \end{bmatrix}. \tag{46}$$

The intent here is to control the viscous numerical fluxes to conserve ‘entropy’ and not to generate more of it. As before, the entropy balance is enforced through the expression:

$$[\mathbf{v}_v]^T \hat{\mathbf{f}}_v - [\mathbf{v}_v \cdot \mathbf{f}_v] = -[F_v] \tag{47a}$$

$$- [2u]\tau^* - [2\tau] \frac{\mu_v}{T_v} u_2^* + [2u\tau^*] + \left[2\tau \frac{\mu_v}{T_v} u_2^* \right] = [2u\tau] \tag{47b}$$

$$- [u]\tau^* - \frac{\mu_v}{T_v} [\tau] u_2^* + \left[\frac{\mu_v}{T_v} \tau u_2^* \right] = 0. \tag{47c}$$

Define the arithmetic averaging as \bar{a} and using the identity $[ab] = \bar{a}[b] + \bar{b}[a]$, the equation expands to

$$- [u]\tau^* - \frac{\mu_v}{T_v} [\tau] u_2^* + \frac{\mu_v}{T_v} ([\tau]\bar{u} + \bar{\tau}[u]) = 0 \tag{48}$$

which gives

$$\tau^* = \frac{\mu_v}{T_v} \bar{\tau}, \quad u_2^* = \bar{u}. \tag{49}$$

Similar to the Burgers’ equation model, the complete discrete fluxes would have the form:

$$\mathbf{f}^* = \hat{\mathbf{f}}_i - \frac{1}{2} \hat{\mathbf{R}}_i |\hat{\mathbf{A}}_i \hat{\mathbf{S}}_i| (\hat{\mathbf{R}}_i)^T [\mathbf{v}_i] + \hat{\mathbf{f}}_v - \frac{1}{2} \hat{\mathbf{R}}_v |\hat{\mathbf{A}}_v \hat{\mathbf{S}}_v| (\hat{\mathbf{R}}_v)^T [\mathbf{v}_v]. \tag{50}$$

These dissipation matrices are diagonalized from their respective flux Jacobians, which is obtained by setting $A = \frac{\partial \mathbf{f}}{\partial \mathbf{u}}$. For the viscous fluxes:

$$\mathbf{A}_v = \frac{\partial \mathbf{f}_v}{\partial \mathbf{u}} = \begin{bmatrix} 0 & 0 & 0 & 0 \\ 0 & 0 & 0 & -1 \\ \frac{\tau u}{\rho} & -\frac{\tau}{\rho} & 0 & -u \\ \frac{u}{\rho} & -\frac{1}{\rho} & 0 & 0 \end{bmatrix} \tag{51}$$

From \mathbf{A}_i and \mathbf{A}_v , the averaged eigenvalues $\hat{\mathbf{A}}_i$ and $\hat{\mathbf{A}}_v$ are calculated to be:

$$\hat{\mathbf{A}}_i = \begin{bmatrix} \hat{u} - \hat{a} & 0 & 0 & 0 \\ 0 & \hat{u} & 0 & 0 \\ 0 & 0 & \hat{u} + \hat{a} & 0 \\ 0 & 0 & 0 & 0 \end{bmatrix}, \quad \hat{\mathbf{A}}_v = \begin{bmatrix} 0 & 0 & 0 & 0 \\ 0 & 0 & 0 & 0 \\ 0 & 0 & -\frac{1}{\rho^{1/2}} & 0 \\ 0 & 0 & 0 & \frac{1}{\rho^{1/2}} \end{bmatrix} \tag{52}$$

The eigenvalues for the inviscid part consist of the two acoustic waves and an entropy wave with the viscous eigenvalues indicating two waves of the same magnitude but travelling in the opposite direction, similar to the eigenvalues in Nishikawa [14]. These two non-zero eigenvalues in the viscous part will contribute to the overall numerical dissipation as in Eq. (50). The components of both sets of eigenvalues consist of entropy-conserved averaged quantities identical to those defined in Ismail and Roe [8]. Alternatively the eigenvalues can be chosen to achieve entropy-consistency following the recommendations from Ismail and Roe [8], where the EC1 and EC2 fluxes therein would be referred to as ECS1 and ECS2 when combined with the hyperbolic system flux in this paper:

$$\hat{\mathbf{A}}_{i,ECS1-NS} = \begin{bmatrix} (\hat{u} - \hat{a}) + \frac{1}{6}|[u - a]| & 0 & 0 & 0 \\ 0 & \hat{u} & 0 & 0 \\ 0 & 0 & (\hat{u} + \hat{a}) + \frac{1}{6}|[u + a]| & 0 \\ 0 & 0 & 0 & 0 \end{bmatrix} \tag{53}$$

$$\hat{\mathbf{A}}_{i,ECS2-NS} = \begin{bmatrix} \beta(\hat{u} - \hat{a}) + \alpha_2|[u - a]| & 0 & 0 & 0 \\ 0 & \hat{u} & 0 & 0 \\ 0 & 0 & \beta(\hat{u} + \hat{a}) + \alpha_2|[u + a]| & 0 \\ 0 & 0 & 0 & 0 \end{bmatrix} \tag{54}$$

In the ECS2 flux, $\beta = 1 + \frac{1}{6}$ and $\alpha_2 = (\alpha_{max} - \alpha_{min})(\max(0, \text{sign}(dM_{max} - [M]))) + \alpha_{min}$, where $\alpha_{max} = 2.0$, $\alpha_{min} = \frac{1}{6}$, and $dM_{max} = 0.5$ It follows that the associated averaged linearly independent right eigenvectors \mathbf{R}_i and \mathbf{R}_v corresponding to the inviscid and viscous eigenvalues are:

$$\hat{\mathbf{R}}_i = \begin{bmatrix} 1 & 1 & 1 & 0 \\ \hat{u} - \hat{a} & \hat{u} & \hat{u} + \hat{a} & 0 \\ \hat{H} - \hat{u}\hat{a} & \frac{1}{2}\hat{u}^2 & \hat{H} + \hat{u}\hat{a} & 0 \\ 0 & 0 & 0 & 0 \end{bmatrix}, \quad \hat{\mathbf{R}}_v = \begin{bmatrix} 0 & \frac{1}{\bar{u}} & 0 & 0 \\ 0 & 1 & \frac{\rho^{1/2}}{\bar{u}} & -\frac{\rho^{1/2}}{\bar{u}} \\ 1 & 0 & \bar{\tau} + \frac{\rho^{1/2}\bar{u}}{\bar{u}} & \bar{\tau} - \frac{\rho^{1/2}\bar{u}}{\bar{u}} \\ 0 & 0 & 1 & 1 \end{bmatrix} \tag{55a}$$

In the viscous set of eigenvectors, the averaged variables $\bar{\tau}$ and \bar{u} are ‘‘entropy-conserving’’ quantities derived from Eq. (49). The inviscid eigenvectors are identical to the one determined by Ismail and Roe [8], excluding the extra row and column of zero-vectors due to the presence of the viscous transport equation.

The first two rows of the viscous dissipation matrix will not affect the overall dissipation since the first two eigenvalues are zero. Thus the viscous scaling matrix are computed such that only the last two rows are determined (the rest are set to zeros) satisfying the differential relations of $\mathbf{R}_v^{-1}d\mathbf{u} = \mathbf{S}_v\mathbf{R}_v^T d\mathbf{v}_v$ as similarly done for the system of Burgers equations. The inviscid scaling matrix S_i are identical to the ones proposed by Ismail and Roe [8] barring the extra column and row of zeros. Thus:

$$\hat{\mathbf{S}}_i = \begin{bmatrix} \frac{\hat{\rho}}{2\gamma} & 0 & 0 & 0 \\ 0 & \frac{(\gamma-1)\hat{\rho}}{\gamma} & 0 & 0 \\ 0 & 0 & \frac{\hat{\rho}}{2\gamma} & 0 \\ 0 & 0 & 0 & 0 \end{bmatrix}, \quad \hat{\mathbf{S}}_v = \begin{bmatrix} 0 & 0 & 0 & 0 \\ 0 & 0 & 0 & 0 \\ K_1 & K_2 & K_3 & K_4 \\ K_2 & K_1 & K_4 & K_3 \end{bmatrix} \tag{56a}$$

where

$$K_1 = \frac{-\rho^{3/2}(\bar{u} + 1)}{4} \tag{57}$$

$$K_2 = \frac{\rho^{3/2}(\bar{u} + 1)}{4} \tag{58}$$

$$K_3 = \frac{(1 + \frac{\bar{u}}{2} - \frac{\bar{\rho}\bar{u}}{2})}{4} \tag{59}$$

$$K_4 = \frac{\bar{u}(\bar{\rho} - 1)}{8}. \tag{60}$$

Variables in the terms of $K_1 - K_4$ are simple arithmetic averaging of the left and right states at each interface.

Since entropy is conserved for both the inviscid and viscous variables, entropy production is generated exclusively from their respective dissipation matrices and their source terms. The

entropy generation of the system can be determined by analysis on each of its components. For the inviscid part:

$$\dot{U}_i = [\mathbf{v}_i]^T \hat{\mathbf{f}}_i - [\rho u] - \frac{1}{2} [\mathbf{v}_i]^T \left(\hat{\mathbf{R}}_i | \hat{\mathbf{A}}_i \hat{\mathbf{S}}_i | \hat{\mathbf{R}}_i^T [\mathbf{v}_i] \right) + \mathbf{v}_i \cdot \mathbf{B} \tag{61a}$$

$$= -\frac{1}{2} \left([\mathbf{v}_i]^T \hat{\mathbf{R}}_i | \hat{\mathbf{A}}_i \hat{\mathbf{S}}_i | \hat{\mathbf{R}}_i^T [\mathbf{v}_i] \right) \tag{61b}$$

$$\leq 0 \tag{61c}$$

Meanwhile, for the viscous part:

$$\dot{U}_v = [\mathbf{v}_v]^T \hat{\mathbf{f}}_v - [\mathbf{v}_v \cdot \mathbf{f}_v] + [F_v] - \frac{1}{2} [\mathbf{v}_v]^T \left(\hat{\mathbf{R}}_v | \hat{\mathbf{A}}_v \hat{\mathbf{S}}_v | \hat{\mathbf{R}}_v^T [\mathbf{v}_v] \right) + \mathbf{v}_v \cdot \mathbf{B} \tag{62a}$$

$$= -\frac{1}{2} \left([\mathbf{v}_v]^T \hat{\mathbf{R}}_v | \hat{\mathbf{A}}_v \hat{\mathbf{S}}_v | \hat{\mathbf{R}}_v^T [\mathbf{v}_v] \right) - 2 \frac{\tau^2}{T_v} \tag{62b}$$

$$\leq 0 \tag{62c}$$

which guarantees entropy stability for the first-order system of Navier–Stokes equations.

4 Results

Results for the entropy consistent systems approach is compiled in this section. For the Burgers’ equation model, the first-order versions of the entropy consistent fluxes, ECS1 and ECS2, are compared with the original EC flux that has been augmented with a central-difference viscosity term as a point of reference. Additionally, the respective exact solutions are included for the cases of steady-shock and the square wave initial condition. On the Navier–Stokes equations, the first-order ESS system flux is compared with its predecessors the ES and EC2 fluxes in the steady shock set-up. A wide range of viscosity coefficients were used for each case, with the Navier–Stokes flux also subjected to variations in Mach number. Furthermore, results for the system flux combined with EC1 and EC2 formulations, named ECS1-NS and ECS2-NS respectively, are also included. Only a few of the results are shown for brevity, but they are still representative of the prevalent trends of the flux behavior.

The calculation for the viscous portion of the system fluxes are done similar to the method used in Nishikawa [14]. For the conventional ES and EC2 fluxes, the central difference scheme was used to resolve viscosity terms. Second-order spatial discretization is performed using limited slope reconstruction, whilst second order time marching is done using the explicit Runge–Kutta method. A summary of abbreviations of the flux functions is available in Table 1.

The CFL limit for stability highly depends on the viscosity-value being used (ν). There are established stability results for the conventional advection–diffusion approach but perhaps it is still in infancy for the hyperbolic-systems approach. Herein we do not intend to rigorously analyze the stability of the hyperbolic-systems approach. However, we observed that (for the most part) the CFL used for the system’s approach is about an order of magnitude larger than for the conventional advection–diffusion approach and still stability is achieved. This somewhat demonstrates the advantages of using a fully hyperbolize advection–diffusion model, though it is not the main aspect of this paper.

Table 1 Abbreviation key of the flux functions tested

No.	Abbreviation	Flux function	Model	Source
1	EC	Entropy consistent scheme	Burgers'	Ismail and Roe [8]
2	ES	Entropy stable scheme	Navier–Stokes	Ismail and Roe [8]
3	EC1	Entropy consistent scheme 1	Navier–Stokes	Ismail and Roe [8]
4	EC2	Entropy consistent scheme 2	Navier–Stokes	Ismail and Roe [8]
5	ECS1	Entropy consistent system 1	Hyp Burgers'	Eqs. (26, 34)
6	ECS2	Entropy consistent system 2	Hyp Burgers'	Eqs. (26, 35)
7	ESS-NS	Entropy stable scheme	Hyp Navier–Stokes	Eqs. (50, 52)
8	ECS1-NS	Entropy consistent system 1	Hyp Navier–Stokes	Eqs. (50, 53)
9	ECS2-NS	Entropy consistent system 2	Hyp Navier–Stokes	Eqs. (50, 54)

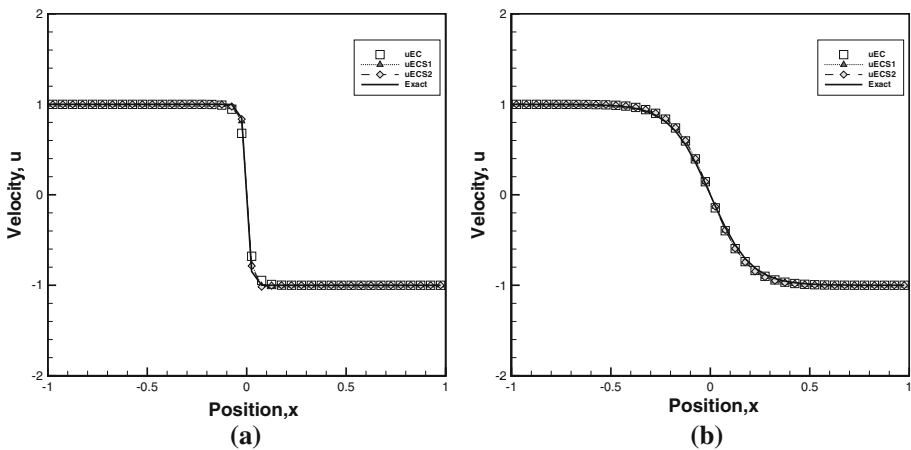


Fig. 1 Steady shock solution for ECS fluxes with **a** $\nu = 10^{-2}$, and **b** $\nu = 10^{-1}$

4.1 Results for Burgers' Equation Model

Steady shock The fluxes are firstly tested on the simple case of steady shock with initial condition of:

$$u(x, 0) = \begin{cases} 1, & \text{if } x < 0 \\ -1, & \text{if } x \geq 0 \end{cases} \tag{63}$$

The exact solution, available in Masatsuka [10], is given by:

$$u = \left(1 - \tanh \frac{x}{2\nu} \right) \tag{64}$$

Results are shown for a viscosity coefficient of 10^{-2} in Fig. 1a, and a viscosity of 10^{-1} in Fig. 1b. In these plots, 40 computational cell were used, but the results remain the same even with finer grid. The boundary conditions on the left and right sides of the domain are of the non-reflecting type.

For the range of viscosity shown, the system fluxes match closely to the benchmark as well as the exact solution. As expected, when the viscosity coefficient is increased, the ECS1 and ECS2 fluxes would become proportionally more diffusive. At the coefficient of $\nu = 10^{-2}$,

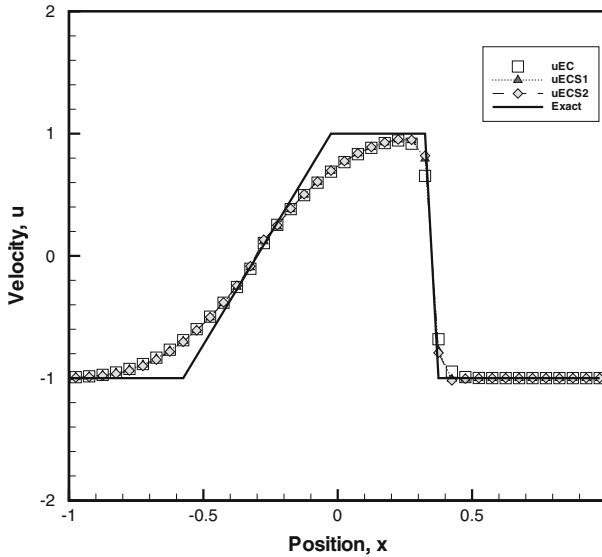


Fig. 2 Solution for square wave initial condition for ECS fluxes with $\nu = 10^{-2}$

we observe that the ECS1 and ECS2 fluxes are marginally less diffusive than the EC. Whilst at the coefficient of $\nu = 10^{-1}$, all the considered fluxes produce similar results. This trend has also been observed in Mohammed and Ismail [11].

The underlying cause that drives these results is in the way each of the flux is constructed. The ECS1 and ECS2 flux’s auxiliary variable that provides diffusion to the system is heavily dependent on the viscosity coefficient to make its presence felt within the system. At low viscosities, the low coefficient value means that the auxiliary term has less influence to the total flux; therefore the ECS1 and ECS2 fluxes provide less dissipation and in turn become a bit closer to the exact solution than the EC flux coupled with a conventional discrete viscosity term.

Square wave A similar, yet more difficult test for the fluxes is performed via the deployment of the square wave initial condition, where:

$$u(x, 0) = \begin{cases} -1, & \text{if } \frac{1}{3} \leq |x| \leq 1 \\ 1, & \text{if } |x| < \frac{1}{3} \end{cases} \tag{65}$$

For conciseness, results are shown for a viscosity coefficient of 10^{-2} . Grid size and boundary conditions are also kept as it was (Fig. 2).

The point of this test case is to see whether the fluxes can avoid capturing the non-physical rarefaction shock, unlike the Roe flux and most other schemes without entropy control. As seen in the plots, the ECS1 and ECS2 fluxes behave similarly to the EC flux around the rarefaction area, which matches the characteristic that we are looking for. The rarefaction fan for all three fluxes are less steep compared to the solution given by the exact Riemann solver in the solid line mostly due to the low CFL number used in the simulation. As for the normal shock region, the ECS1 and ECS2 fluxes exhibit a similar diffusive pattern to the previous case, with the ECS1 flux being the least diffusive, and the EC flux the most diffusive.

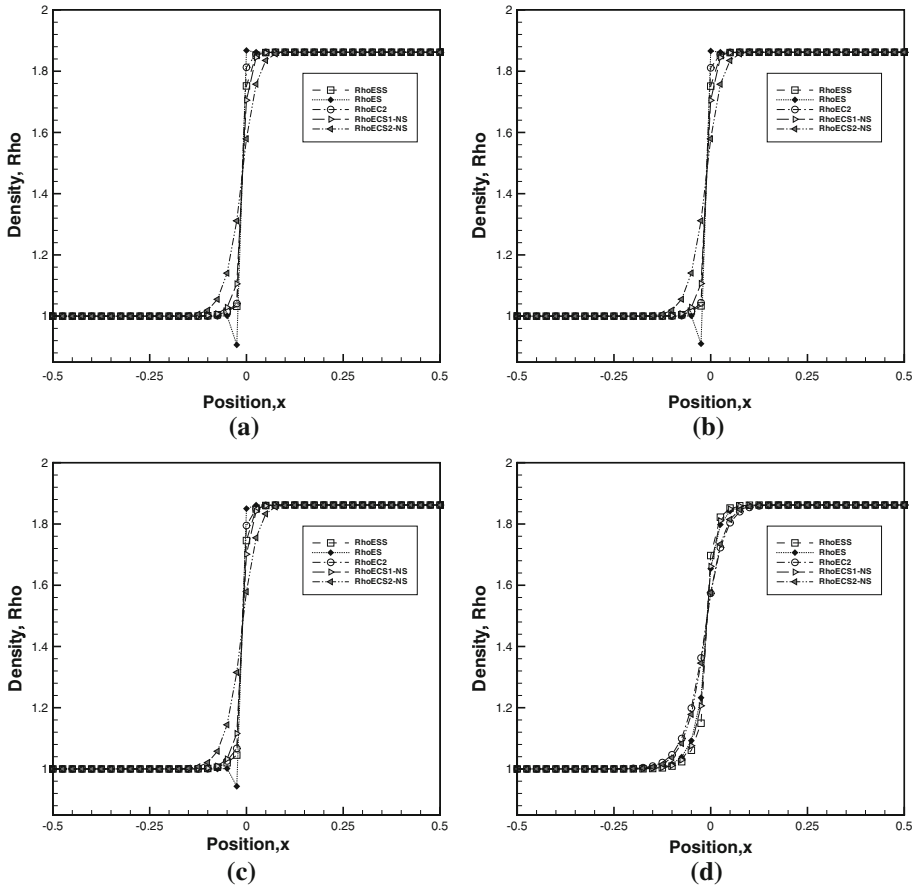


Fig. 3 Density plot of steady shock for the fluxes at Mach 1.5 with viscosity of **a** $1e-7$, **b** $1e-4$, **c** $1e-3$, and **d** $1e-2$

4.2 Results for Navier–Stokes Equation Model

Steady shock Next, the first order system approach is applied in modelling the Navier–Stokes equations. Similar to Burgers’, the flux is initially tested in the case of steady-state shock with the Rankine–Hugoniot initial condition:

$$\mathbf{u}_0 = \left[f(M_0) \quad 1 \quad \frac{g(M_0)}{\gamma(\gamma - 1)M_0^2} + \frac{1}{2f(M_0)} \right] \tag{66a}$$

$$f(M_0) = \left(\frac{2}{(\gamma + 1)M_0^2} + \frac{\gamma - 1}{\gamma + 1} \right)^{-1} \tag{66b}$$

$$g(M_0) = \frac{2\gamma M_0^2}{\gamma + 1} - \frac{\gamma - 1}{\gamma + 1} \tag{66c}$$

$$\mathbf{u}_1 = \left[1 \quad 1 \quad \frac{1}{\gamma(\gamma - 1)M_0^2} + \frac{1}{2} \right] \tag{66d}$$

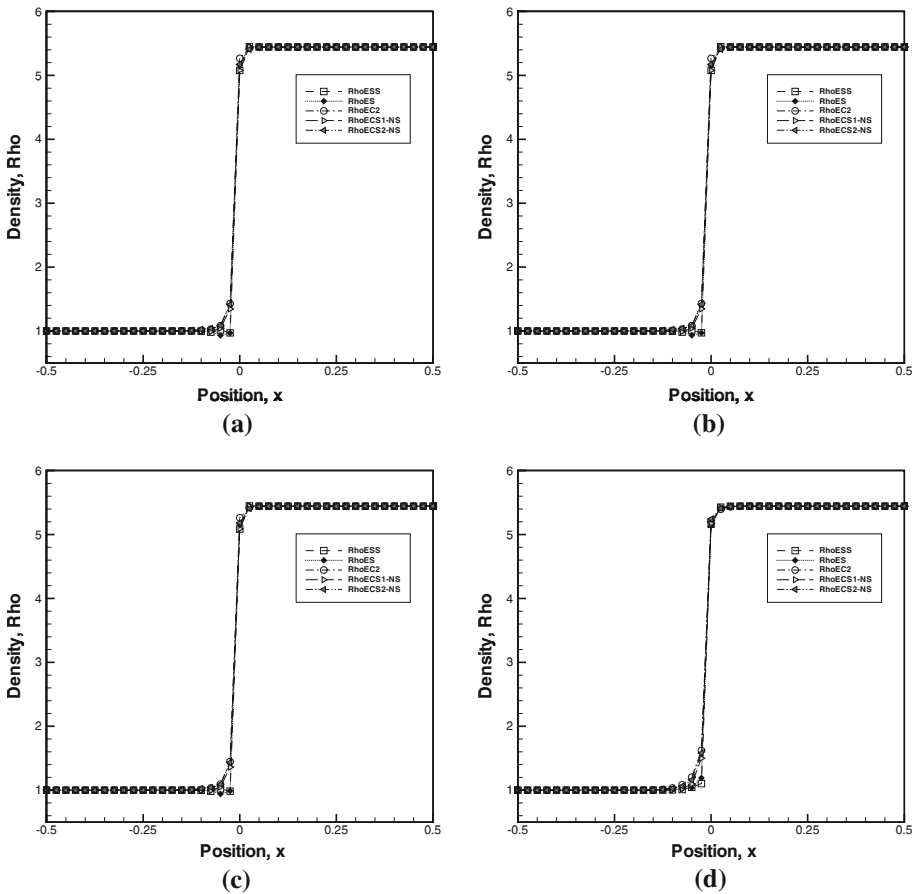


Fig. 4 Density plot of steady shock for the fluxes at Mach 7.0 with viscosity of **a** $1e-7$, **b** $1e-4$, **c** $1e-3$, and **d** $1e-2$

The system flux (ESS) is then compared to its predecessors, which are the entropy stable (ES) flux, and the entropy consistent fluxes of EC1 and EC2 available from Ismail and Roe [8]. The ES, EC1, and EC2 fluxes are originally derived for the Euler equations; they are modified here to include central-difference physical viscosity terms that account for viscous stresses, making them essentially Navier–Stokes equation models. Additionally, results for the ESS flux combined with the EC1 and EC2 formulation, designated as ECS1-NS and ECS2-NS respectively, has also been included. Density plots of the said fluxes is shown in Fig. 3 for a Mach number of $Ma = 1.5$, Fig. 4 for a Mach number of $Ma = 7.0$, and Fig. 5 for a Mach number of $Ma = 20.0$. In Fig. 3b, the exact solution for density is given by [20] at a viscosity value of 0.00025. A summary of the figures for the results is available in Table 2.

At low Mach number and low to medium viscosities (Fig. 3a–c), the ESS flux is closer to the EC1 and EC2 fluxes as opposed to the ES flux. The ESS flux exhibit very little undershoot even at the lowest viscosity setting. The result is significant since the EC1 and EC2 have the third entropy production term built in to them, whilst the ECS flux relies only on the entropy-stable term to provide diffusion. On the other hand, the ESS flux is less diffusive

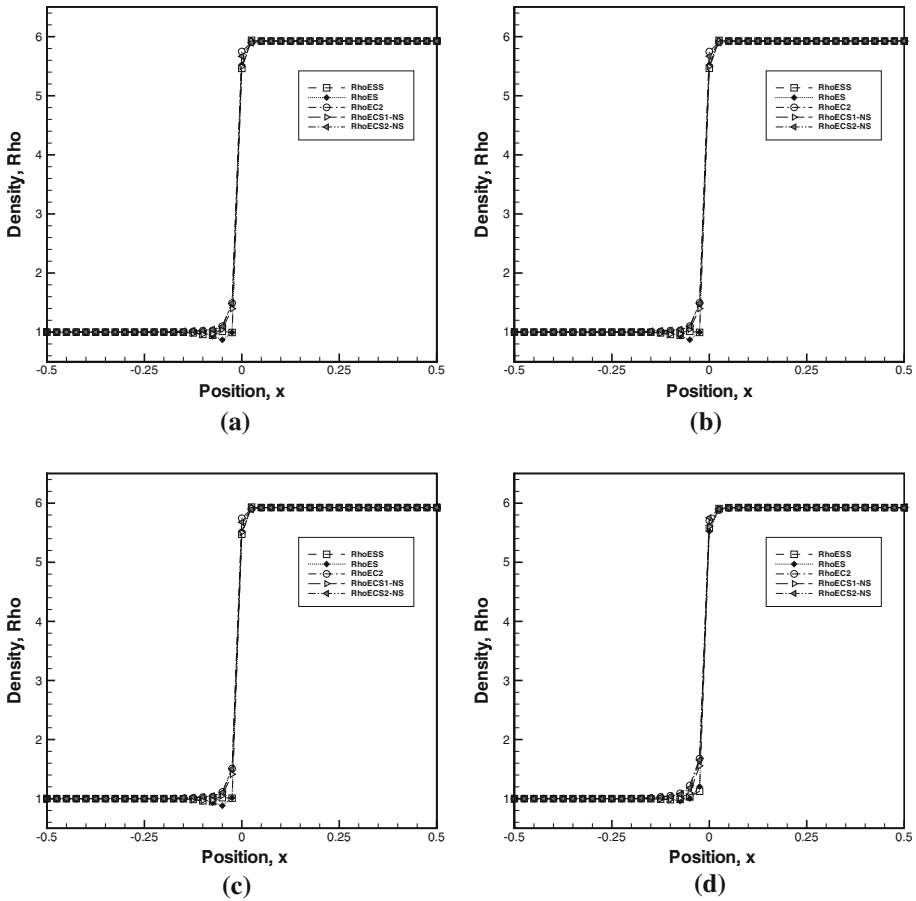


Fig. 5 Density plot of steady shock for the fluxes at Mach 20.0 with viscosity of **a** $1e - 7$, **b** $1e - 4$, **c** $1e - 3$, and **d** $1e - 2$

Table 2 Summary of figures detailing the result of the Navier–Stokes fluxes

	$Ma = 1.5$	$Ma = 7.0$	$Ma = 20.0$
$\nu = 1.0 \times 10^{-7}$	Figure 3a	Figure 4a	Figure 5a
$\nu = 1.0 \times 10^{-4}$	Figure 3b	Figure 4b	Figure 5b
$\nu = 1.0 \times 10^{-3}$	Figure 3c	Figure 4c	Figure 5c
$\nu = 1.0 \times 10^{-2}$	Figure 3d	Figure 4d	Figure 5d

than others at high viscosity, as seen in Fig. 3d. In this condition, the ESS flux is closer to the ES and EC1 flux compared to EC2, suggesting that the ECS flux would be less susceptible to problems related to over-diffusion. Additionally, the ECS1-NS and ECS2-NS fluxes are also found to be less diffusive than their conventional counterpart EC2. Perhaps this is due to the overall diffusion process based on wave-characteristics for the hyperbolic-systems which is known to be minimally diffusive. However, ECS1-NS and ECS2-NS are more diffusive than the ESS method (Fig. 6).

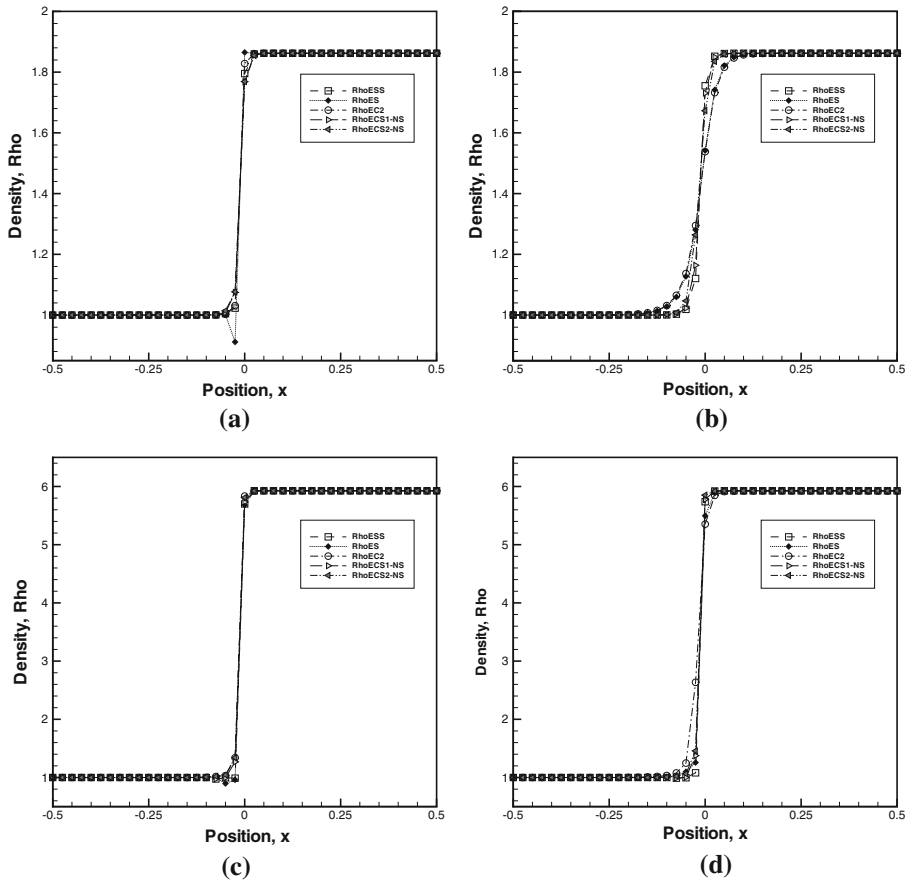


Fig. 6 Second order density plot of steady shock for the fluxes in the case of **a** $Ma = 1.5, \nu = 1e - 7$, **b** $Ma = 1.5, \nu = 1e - 2$, **c** $Ma = 20.0, \nu = 1e - 7$, and **d** $Ma = 20.0, \nu = 1e - 2$

The pattern becomes a little different as the Mach number is increased as in Figs. 4 and 5. In the said plots, the EC2 flux can be seen as being significantly more diffused than the other ones. This is most probably due to the the additional entropy production of the EC2 flux being dependent on Mach number. The ESS is observed to still have a small amount of undershoot at low viscosity, but the undershoot is a bit less than the ES flux. The undershoot is gradually decreased as the viscosity coefficient value is increased. At high viscosity, the ESS flux is comparable to the EC1 flux. Again, the ECS1-NS and ECS2-NS fluxes are a little more diffusive than ESS, but less so than EC2. Overall, the dependence on numerical viscosity to achieve entropy–consistency is less when the physical viscosity is increased.

5 Concluding Remarks

The first-order hyperbolic systems approach has been incorporated with elements of entropy stability and consistency to create new flux functions. For the Burgers’ equation model, a new entropy pair has been chosen to include both inviscid and viscous terms. For the fluxes

approximating the Navier–Stokes equations, hyperbolic discretization of viscosity terms is done separately from inviscid terms so that the physical (or mathematical) entropy still remains a dominant feature for the overall entropy–stability and entropy–consistency control. The additional entropy function for the viscous terms are created to ensure some form of entropy–stability is also achieved for hyperbolic discretization of the physical viscosity. The new fluxes have been shown to provide comparable results to older methods for a range of viscosity levels. However, the Navier–Stokes fluxes are still incomplete due to the omission of heat transfer effects. Due to their respective signs, the entropy generation from heat transfer would oppose that of the rest of the system, affecting the entropy stability and consistency of the system as a whole. Thus, considerable work is still required to explore the full potential of this approach.

Acknowledgments This research is made possible in part by Universiti Sains Malaysia Research University Grant (No: 1001/PAERO/814152), Universiti Tun Hussein Onn Malaysia and scholarship from the Malaysian Ministry of Higher Education.

Appendix 1: Entropy Conserving Flux

The entropy conserving flux \mathbf{f}_i from Eq. (50) satisfies

$$\mathbf{v}^T \mathbf{f}_i = [\rho u] \tag{67}$$

and is calculated based on averaged quantities of

$$\mathbf{f}_i(\mathbf{u}_L, \mathbf{u}_R) = \begin{bmatrix} \hat{\rho} \hat{u} \\ \hat{\rho} \hat{u}^2 + \hat{p}_1 \\ \hat{\rho} \hat{u} \hat{H} \end{bmatrix} \tag{68}$$

To determine the averaged quantities, we firstly define $z_1 = \sqrt{\frac{\rho}{p}}$, $z_2 = \sqrt{\frac{\rho}{p} u}$, $z_3 = \sqrt{\rho p}$. The averaged quantities are composed from functions of arithmetic mean $\bar{a} = \frac{a_L + a_R}{2}$ and logarithmic mean as defined in “Appendix 2”. Based on Eq. (67), the quantities used in the flux are as follows

$$\hat{u} = \frac{\bar{z}_2}{\bar{z}_1}, \quad \hat{\rho} = \bar{z}_1 \bar{z}_3^{ln}, \quad \hat{p}_1 = \frac{\bar{z}_3}{\bar{z}_1}, \quad \hat{p}_2 = \frac{\gamma + 1}{2\gamma} \frac{z_3^{ln}}{z_1^{ln}} + \frac{\gamma - 1}{2\gamma} \frac{\bar{z}_3}{\bar{z}_1} \tag{69}$$

$$\hat{a} = \left(\frac{\gamma \hat{p}_2}{\hat{\rho}} \right)^{\frac{1}{2}}, \quad \hat{H} = \frac{\hat{a}^2}{\gamma - 1} + \frac{\hat{u}^2}{2} \tag{70}$$

Appendix 2: Logarithmic Mean

Let $\zeta = \frac{a_L}{a_R}$. Define $a^{ln}(L, R) = \frac{a_L + a_R}{ln(\zeta)} \frac{\zeta - 1}{\zeta + 1}$ where $ln(\zeta) = 2\left(\frac{1-\zeta}{1+\zeta} + \frac{1}{3} \frac{(1-\zeta)^3}{(1+\zeta)^3} + \frac{1}{5} \frac{(1-\zeta)^5}{(1+\zeta)^5} + \frac{1}{7} \frac{(1-\zeta)^7}{(1+\zeta)^7} + O(\zeta^9)\right)$. To calculate the logarithmic mean we use the following subroutine:

1. Set the following: $\zeta = \frac{a_L}{a_R}$, $f = \frac{\zeta - 1}{\zeta + 1}$, $u = f * f$
2. If $(u < \epsilon)$

$$F = 1.0 + u/3.0 + u * u/5.0 + u * u * u/7.0$$

3. Else

$$F = \ln(\zeta)/2.0/(f)$$

thus

$$a^{\ln(L, R)} = \frac{aL + aR}{2F}, \quad \epsilon = 10^{-2}$$

References

- Barth, T.J.: Numerical methods for gasdynamic systems on unstructured meshes. In: Kroner, M.O.D., Rhode, C. (eds.) *An Introduction to Recent Developments in Theory and Numerics for Conservation Laws*, pp. 195–285. Springer (1999). Lect. Notes Comput. Sci. Eng. 5
- Fjordholm, U.S., Mishra, S., Tadmor, E.: Energy preserving and energy stable schemes for the shallow water equations. In: *Foundations of Computational Mathematics Hong Kong 2008*, pp. 93–139. Cambridge University Press (2008). London Mathematical Society Lecture Note Series 363
- Fjordholm, U.S., Mishra, S., Tadmor, E.: Energy stable schemes well-balanced schemes for the shallow water equations with bottom topography. *J. Comput. Phys.* **230**, 5587–5609 (2011)
- Fjordholm, U.S., Mishra, S., Tadmor, E.: Arbitrarily high-order accurate entropy stable essentially non-oscillatory schemes for systems of conservation laws. *SIAM J. Numer. Anal.* **50**, 544–573 (2012)
- Fjordholm, U.S., Mishra, S., Tadmor, E.: Eno reconstruction and eno interpolation are stable. *Found. Comput. Math* **13**, 139–159 (2013)
- Hughes, T., Franca, L., Mallet, M.: A new finite element formulation for compressible fluid dynamics i: symmetric forms of the compressible Euler and Navier–Stokes equations and the second law of thermodynamics. *Comput. Methods Appl. Mech. Eng.* **54**, 223–234 (1986)
- Ismail, F.: Toward a reliable prediction of shocks in hypersonic flow: resolving carbuncles with entropy and vorticity control. Ph.D. Thesis, The University of Michigan (2006)
- Ismail, F., Roe, P.L.: Affordable, entropy consistent Euler flux functions II: entropy production at shocks. *J. Comput. Phys.* **228**, 5410–5436 (2009)
- Kitamura, K., Roe, P., Ismail, F.: An evaluation of Euler fluxes for hypersonic computations, 2007-4465. AIAA Conference, Miami (2007)
- Masatsuka, K.: I do like CFD, VOL. 1. *Governing Equations and Exact Solutions*, first edn. Katate Masatsuka (2009)
- Mohammed, A.N., Ismail, F.: Study of an entropy-consistent Navier–Stokes flux. *Int. J. Comput. Fluid Dyn.* **27**, 1–14 (2013)
- Nishikawa, H.: A first-order system approach for diffusion equation. I: second-order residual-distribution schemes. *J. Comput. Phys.* **227**, 315–352 (2007)
- Nishikawa, H.: A first-order system approach for diffusion equation. II: unification of advection and diffusion. *J. Comput. Phys.* **229**, 3989–4016 (2010)
- Nishikawa, H.: New-generation hyperbolic navier-stokes schemes: $O(1/h)$ speed-up and accurate viscous/heat fluxes. In: *20th AIAA CFD Conference*, pp. AIAA Paper 2011–3043. AIAA Conferences, Hawaii (2011)
- Nishikawa, H.: First, second, and third order finite-volume schemes for navier-stokes equations. In: *7th AIAA Theoretical Fluid Mechanics Conference*, pp. AIAA Paper 2014–2091. AIAA Conferences, Atlanta, Georgia (2014)
- Roe, P.L.: Affordable, entropy-consistent, Euler flux functions I: analytical results. unpublished (unpublished)
- Tadmor, E.: The numerical viscosity of entropy stable schemes for systems of conservation laws. *Math. Comput.* **49**, 91–103 (1987)
- Tadmor, E., Zhong, W.: Novel entropy stable schemes for 1D and 2D fluid equations. In: Benzoni-Gavage, S., Serre, D. (eds.) *11th International Conference Hyperbolic Problems: Theory, Numerics, Applications*
- Tadmor, E., Zhong, W.: Entropy stable approximations of navier-stokes equations with no artificial numerical viscosity. *J. Hyperb. DE* **3**, 529–559 (2006)
- Xu, K.: Gas kinetic schemes for fluid simulations. In: Satofuka, N. (ed.) *1st International Conference on Computational Fluid Dynamics*, pp. 14–23. Kyoto, Japan (2000)